Article

Titration *in Silico* of Reversible B A Transitions in DNA

Alexey K. Mazur

J. Am. Chem. Soc., **2003**, 125 (26), 7849-7859• DOI: 10.1021/ja034550j • Publication Date (Web): 05 June 2003

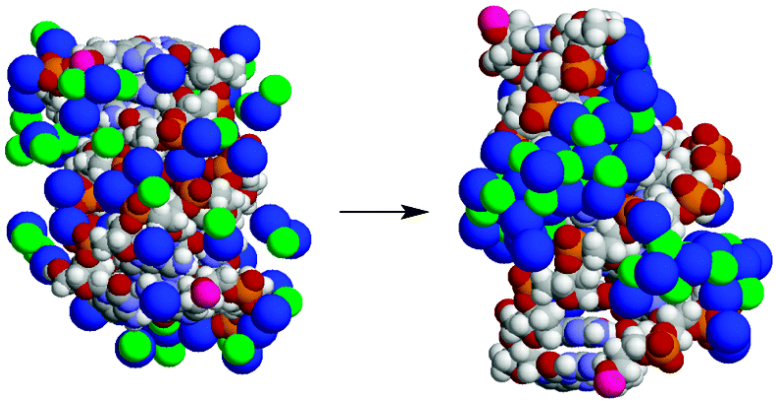

J|A|C|S
ARTICLES
Published on Web 06/05/2003

Titration *in Silico* of Reversible B ↔ A Transitions in DNA

Alexey K. Mazur

Contribution from the Laboratoire de Biochimie Théorique, CNRS UPR9080, Institut de Biologie Physico-Chimique 13, rue Pierre et Marie Curie, Paris 75005, France

Received February 7, 2003; E-mail: alexey@ibpc.fr

Abstract: Reversible transitions between the A- and B-forms of DNA are obtained in free molecular dynamics simulations of a single double helix immersed in a water drop with Na^+ counterions. The dynamics of the transitions agrees with their supposed cooperative character. *In silico* titration of the transitions was carried out by smooth variation of the drop size. The estimated range of hydration numbers corresponding to the transition roughly agrees with experimental data. The chain length dependence was studied for double helices from 6 to 16 base pairs. It appeared that the B → A transition is hindered for DNA shorter than one helical turn. With increased NaCl concentration in the drop, stabilization of the B-form is observed accompanied by the salt crystallization. The results strongly suggest that the B → A transition at low hydration is caused by Na^+ ions sandwiched between phosphate strands in the major groove and is driven by direct medium range electrostatic interactions. The role of the reduced water shell apparently consists of increasing the counterion concentration in the opening of the major groove. Analysis of the available experimental data suggests that this mechanism is perhaps generally responsible for the A/B polymorphism in DNA.

Introduction

The transformation from B-DNA[1] to dehydrated A-DNA[2] in fibers was one of the first reversible structural transitions observed in a biomolecule. These structures represent right-handed helical duplexes with identical topologies and hydrogen bonding, and yet they have strongly different shapes.[3,4] The B-helix is long and narrow, with stacked base pairs forming the core of the helix. In contrast, the A-DNA structure is short and thick, with strongly inclined base pairs wrapping around a 6 Å solvent accessible cylindrical hole. The B-form is the dominant biological conformation of DNA, whereas the A-form is considered as a high energy state that some sequences can adopt temporarily during various biological functions.[5] Indeed, local A-DNA motives are rather common in crystal structures of protein−DNA complexes.[6,7] The A ↔ B polymorphism is currently considered as one of the modes for governing protein−DNA interactions.[8]

A complete B → A transition in a long mixed sequence DNA can be obtained *in vitro* in a few special conditions. In crystalline[2,9] and amorphous[10] fibers as well as in films,[11] it is induced by equilibrating the samples under reduced relative humidity or with the concentration of organic solvents increased to ∼80%.[12] Organic solvents can also provoke B → A transition in an isolated DNA molecule in solution.[13] The transition is reversible and cooperative,[14,15] which means that it occurs concertedly in an extended DNA fragment rather than randomly in separate nucleotides. The characteristic length of such a fragment, however, is rather small. Originally, it was estimated as 20 base pairs,[15] but later this estimate was reduced to 10 base pairs,[13] that is, approximately one helical turn. DNA fragments shorter than this length generally do not go to the A-form in solution.[16,17] For some sequences, however, short DNA fragments could be crystallized in the A-form.[18,19] Under physiological conditions *in vitro*, the A/B balance depends on the environment, notably, the types of solvent counterions[14] and the temperature.[20] It is also sequence dependent, with some sequences exhibiting in solution the features of both forms.[16,21,22] The transition is significantly facilitated in groups of consecutive guanines (G-tracts), whereas in A-tracts it is more difficult.[9,23,24]

(1) Watson, J. D.; Crick, F. H. C. *Nature* **1953**, *171*, 737−738.
(2) Franklin, R. E.; Gosling, R. G. *Nature* **1953**, *171*, 740−741.
(3) Saenger, W. *Principles of Nucleic Acid Structure*; Springer-Verlag: New York, 1984.
(4) Calladine, C. R.; Drew, H. R. *Understanding DNA: The Molecule & How it Works*; Academic Press: London, 1992.
(5) Ivanov, V. I.; Minchenkova, L. E. *Mol. Biol.* **1995**, *28*, 780−788.
(6) Timsit, Y. *J. Mol. Biol.* **1999**, *293*, 835−853.
(7) Lu, X. J.; Shakked, Z.; Olson, W. K. *J. Mol. Biol.* **2000**, *300*, 819−840.
(8) Ng, H.-L.; Kopka, M. L.; Dickerson, R. E. *Proc. Natl. Acad. Sci. U.S.A.* **2000**, *97*, 2035−2039.
(9) Leslie, A. G. W.; Arnott, S.; Chandrasekaran, R.; Ratliff, R. L. *J. Mol. Biol.* **1980**, *143*, 49−72.
(10) Piskur, J.; Rupprecht, A. *FEBS Lett.* **1995**, *375*, 174−178.
(11) Tunis-Schneider, M. J.; Maestre, M. F. *J. Mol. Biol.* **1970**, *52*, 521−541.
(12) Zimmerman, S. B.; Pheiffer, B. H. *Cold Spring Harbor Symp. Quant. Biol.* **1983**, *47*, 67−76.
(13) Ivanov, V. I.; Minchenkova, L. E.; Minyat, E. E.; Schyolkina, A. K. *Cold Spring Harbor Symp. Quant. Biol.* **1983**, *47*, 243−250.
(14) Ivanov, V. I.; Minchenkova, L. E.; Schyolkina, A. K.; Poletaev, A. I. *Biopolymers* **1973**, *12*, 89−110.
(15) Ivanov, V. I.; Minchenkova, L. E.; Minyat, E. E.; Frank-Kametetskii, M. D.; Schyolkina, A. K. *J. Mol. Biol.* **1974**, *87*, 817−833.
(16) Fairall, L.; Martin, S.; Rhodes, D. *EMBO J.* **1989**, *8*, 1809−1817.
(17) Galat, A. *Eur. Biophys. J.* **1990**, *17*, 331−342.
(18) Conner, B. N.; Takano, T.; Tanaka, S.; Itakura, K.; Dickerson, R. E. *Nature* **1982**, *295*, 294−299.
(19) Wahl, M. C.; Sundaralingam, M. In *Oxford Handbook of Nucleic Acid Structure*; Neidle, S., Ed.; Oxford University Press: New York, 1999; pp 117−144.
(20) Nishimura, Y.; Torigoe, C.; Tsuboi, M. *Nucleic Acids Res.* **1986**, *14*, 2737−2749.
(21) Wolk, S.; Thurmes, W. N.; Ross, W. S.; Hardin, C. C.; Tinoco, I., Jr. *Biochemistry* **1989**, *28*, 2452−4259.
(22) Lindqvist, M.; Gräslund, A. *J. Mol. Biol.* **2001**, *314*, 423−432.

The A/B-philicity of different base pair steps and triplets has been parametrized and used successfully for predicting the properties of mixed sequences.[5,25,26]

Several different ideas concerning detailed molecular aspects and the driving forces of A ↔ B transitions in DNA were discussed in different years.[4,14,27−33] Both the sugar phosphate backbone[29] and base pair stacking[28] were proposed as one of the possible actors in the transition, with water as an evident second partner. Water bridges between certain DNA atoms may stabilize either B-DNA[28] or A-DNA,[29] and the hydrophobic effect possibly favors a B-DNA type of stacking.[14,30] It has been suggested that the reduced water activity is a universal factor that shifts the equilibrium toward A-DNA,[34] which was later replaced by a less specific "economics of hydration".[29] Although the B → A transition induced by increased salt concentration has been reported for poly-dG,[20] the low water activity in high salt generally does not induce B → A transitions.[14,35] In any case, it is not clear how the reduced amount of water around DNA affects its structure at the atomic level.[36] B → A transitions in G-tract duplexes are also induced by polyamine cations bound specifically to N7 and O6 guanine atoms in the major groove,[37−39] and this effect was reproduced in MD simulations.[32] Already early electrostatic calculations showed that the major groove of the A-form is a strong low potential zone,[40] and recent experimental[41] and simulation[31] results suggest that accumulation of metal cations here may be involved in the general mechanism of B → A transitions.

The cooperativity of the B → A transition is poorly understood. Its physical origin was initially attributed to the sugar puckering.[14,15] The furanose ring conformation is C3′-endo (north) in A-DNA (with the C3′-carbon puckered above the furanose plane toward the nucleobase) and C2′-endo (south) in B-DNA.[3] For a single nucleoside in a vacuum, the C2′-endo conformation is slightly lower in energy, with the barrier of 2−3 kcal/mol between the two states,[42] and this is the only significant local energy barrier between the A- and B-DNA conformations. Until recently, it was assumed that the switch in the sugar pucker is strictly linked with the base pair orientation. The latter is restrained due to stacking interactions with the neighbors; therefore, the sugar conformations can change only simultaneously in at least several consecutive base pairs. These views, however, were always questioned,[28] and the recent X-ray and spectroscopic studies really demonstrated that the north sugar puckers are accessible without the B → A transition.[16,21,22] Even with all sugars in the C3′-endo conformation, base pair orientations can strongly differ from the canonical A-form, notably, as regards the rise and inclination,[8] which means that the structure may well be recognized as B-DNA by solution circular dichroism.[43]

It appears, therefore, that the sugar conformations are only weakly restrained by the stacking and the observed cooperativity can hardly be due to the sugar pseudorotation barrier. At the same time, the ensemble of the currently available X-ray DNA structures agrees with the cooperative character of the B → A transition. Although some A-DNA structures have B-like features near the termini,[44] and there exist a series of structures classified as A/B transition intermediates,[45] the A- and B-forms generally do not mix in the same DNA fragment. The two forms may even coexist in a crystal but in different samples of the same fragment.[46]

Many aspects of the A/B polymorphism were earlier studied by theoretical methods. Its thermodynamics is well described by an analytical theory based upon the Ising model.[15] Reduced[28,30,47] and all atom[48] models in continuous dielectric were used for studying its mechanism and sequence dependence. On the other hand, different analytical theories combined with simplified DNA representation were used for modeling solvent effects.[49] Steady progress in MD simulations of DNA since the pioneering calculations by Levitt[50] recently made possible detailed modeling of A/B transitions in a realistic environment including explicit water and metal counterions.[31−33,51−56] They shed new light upon the putative molecular mechanisms involved in the DNA A/B polymorphism despite the limited time of MD trajectories and some force field artifacts.[57]

In the present study, I try to gain new insight in this problem by using a different MD approach. It has recently been shown that the particle-mesh Ewald (PME) algorithm allows one to follow the dynamics of a DNA double helix put in a small salty water drop.[58] An evident question one asks is what happens if the size of the drop is reduced? It is found here that a transition from B- to A-form is reproducibly observed in small water drops

(23) Peticolas, W. L.; Wang, Y.; Thomas, G. A. *Proc. Natl. Acad. Sci. U.S.A.* **1988**, *85*, 2579−2583.
(24) Ivanov, V. I.; Minchenkova, L. E.; Burckhardt, G.; Birch-Hirschfeld, E.; Fritzsche, H.; Zimmer, C. *Biophys. J.* **1996**, *71*, 3344−3349.
(25) Basham, B.; Schroth, G. P.; Ho, P. S. *Proc. Natl. Acad. Sci. U.S.A.* **1995**, *92*, 6464−6468.
(26) Tolstorukov, M. Y.; Ivanov, V. I.; Malenkov, G. G.; Jernigan, R. L.; Zhurkin, V. B. *Biophys. J.* **2001**, *81*, 3409−3421.
(27) Alden, C. J.; Kim, S.-H. *J. Mol. Biol.* **1979**, *132*, 411−434.
(28) Calladine, C. R.; Drew, H. R. *J. Mol. Biol.* **1984**, *178*, 773−782.
(29) Saenger, W.; Hunter, W. N.; Kennard, O. *Nature* **1986**, *324*, 385−388.
(30) Hunter, C. A. *J. Mol. Biol.* **1993**, *230*, 1025−1054.
(31) Cheatham, T. E., III; Crowley, M. F.; Fox, T.; Kollman, P. A. *Proc. Natl. Acad. Sci. U.S.A.* **1997**, *94*, 9626−9630.
(32) Cheatham, T. E., III; Kollman, P. A. *Structure* **1997**, *5*, 1297−1311.
(33) Jayaram, B.; Sprous, D.; Young, M. A.; Beveridge, D. L. *J. Am. Chem. Soc.* **1998**, *120*, 10629−10633.
(34) Malenkov, G.; Minchenkova, L.; Minyat, E.; Schyolkina, A.; Ivanov, V. *FEBS Lett* **1975**, *51*, 38−42.
(35) Zimmerman, S. B.; Pheiffer, B. H. *J. Mol. Biol.* **1980**, *142*, 315−330.
(36) Fuller, W.; Mahensdasingam, A.; Forsyth, V. T. *Nature* **1988**, *335*, 596.
(37) Xu, Q.; Shoemaker, R. K.; Braunlin, W. H. *Biophys. J.* **1993**, *65*, 1039−1049.
(38) Xu, Q.; Jampani, S. R.; Braunlin, W. H. *Biochemistry* **1993**, *32*, 11754−11760.
(39) Robinson, H.; Wang, A. H.-J. *Nucleic Acids Res.* **1996**, *24*, 676−682.
(40) Lavery, R.; Pullman, B. *Nucleic Acids Res.* **1981**, *9*, 4677−4688.
(41) Robinson, H.; Gao, Y.-G.; Sanishvili, R.; Joachimiak, A.; Wang, A. H.-J. *Nucleic Acids Res.* **2000**, *28*, 1760−1766.
(42) Foloppe, N.; Nilsson, L.; MacKerell, A. E., Jr. *Biopolymers* **1999**, *61*, 61−76.
(43) Johnson, B. B.; Dahl, K. S.; Tinoco, I., Jr.; Ivanov, V. I.; Zhurkin, V. B. *Biochemistry* **1981**, *20*, 73−78.
(44) Malinina, L.; Fernandez, L. G.; Huynh-Dinh, T.; Subirana, J. A. *J. Mol. Biol.* **1999**, *285*, 1679−1690.
(45) Vargason, J. M.; Henderson, K.; Ho, P. S. *Proc. Natl. Acad. Sci. U.S.A.* **2001**, *98*, 7265−7270.
(46) Doucet, J.; Benoit, J.-P.; Cruse, W. B.; Prange, T.; Kennard, O. *Nature* **1989**, *337*, 190−192.
(47) Mazur, J.; Sarai, A.; Jernigan, R. L. *Biopolymers* **1989**, *28*, 1223−1233.
(48) Ivanov, V. I.; Zhurkin, V. B.; Zavriev, S. K.; Lysov, Y. P.; Minchenkova, L. E.; Minyat, E. E.; Frank-Kamenetskii, M. D.; Schyolkina, A. K. *Int. J. Quantum Chem.* **1979**, *16*, 189−201.
(49) Jayaram, B.; Beveridge, D. L. *Annu. Rev. Biophys. Biomol. Struct.* **1996**, *25*, 367−394.
(50) Levitt, M. *Cold Spring Harbor Symp. Quant. Biol.* **1983**, *47*, 251−262.
(51) Cheatham, T. E., III; Kollman, P. A. *J. Mol. Biol.* **1996**, *259*, 434−444.
(52) Yang, L.; Pettitt, B. M. *J. Phys. Chem. B* **1996**, *100*, 2564−2566.
(53) Cieplak, P.; Cheatham, T. E., III; Kollman, P. A. *J. Am. Chem. Soc.* **1997**, *119*, 6722−6730.
(54) Sprous, D.; Young, M. A.; Beveridge, D. L. *J. Phys. Chem. B* **1998**, *102*, 4658−4667.
(55) Langley, D. R. *J. Biomol. Struct. Dyn.* **1998**, *16*, 487−509.
(56) Soliva, R.; Luque, F. J.; Alhambra, C.; Orozco, M. *J. Biomol. Struct. Dyn.* **1999**, *17*, 89−99.
(57) Feig, M.; Pettitt, B. M. *Biophys. J.* **1998**, *75*, 134−149.
(58) Mazur, A. K. *J. Am. Chem. Soc.* **2002**, *124*, 14707−14715.

starting from a certain limiting size and that an opposite transition occurs in larger drops. A small water shell around a single double helix can result from water evaporation; therefore, these conditions resemble those in dried fiber samples where the B/A polymorphism was first discovered.[1,2] The effect turns out to be reversible in the nanosecond time scale, which makes possible testing different hypotheses concerning its mechanism. The MD simulations suggest that the A ↔ B polymorphism in an isolated water drop results from a subtle interplay between counterions and the limited water shell around the DNA molecule. The transitions are mainly driven by medium range electrostatic interactions between DNA backbone and counterions accumulated in the major groove. Evidence suggests that in other conditions such transitions may be actually governed by the same mechanism.

Our calculations give the best currently possible prediction of the properties of isolated DNA molecules in salty water drops. One should note that the present approach is fundamentally different from the early DNA simulations where limited water shells were employed to reduce the system size and avoid interactions between periodical images.[59−61] In those cases, the water shells had to reproduce the bulk environment conditions, and special boundary potentials were proposed to correct for strong positional and orientation effects at the water drop surface.[62−64] In contrast, here the surface effects are considered as essential physical factors inherent in the model system, and it is assumed that the force field employed is able to reproduce them.

Methods

In the series MD simulations presented here, the Dickerson−Drew double helical dodecamer (CGCGAATTCGCG[65]) and its derivatives are used as examples. Similar results were also observed for several other test sequences. This particular DNA fragment is preferred because it is neither A-philic or B-philic and because its dynamic structure with Cornell et al. force field[66] is rather close to experimental data.[53,67,68] The simulation protocols were similar to the earlier water drop simulations.[58] We use the internal coordinate molecular dynamics (ICMD) method[69,70] adapted for DNA[71,72] with the time step of 0.01 ps. In this approach, the DNA molecule has all bond lengths and almost all bond angles fixed at their standard values. The only variable bond angles are those centered at the sugar C1′,...,C4′, and O4′ atoms, which ensures the flexibility of the furanose rings. In contrast, bases, thymine methyls, and phosphate groups move as articulated rigid bodies, with only rotations around single bonds allowed. The highest frequencies in thus obtained models are additionally balanced by increasing rotational inertia of the lightest rigid bodies as described earlier.[73,71] The possible physical effects of the above modifications have been discussed elsewhere.[70,74] The electrostatic interactions are evaluated with the shifted Coulomb law by using the smooth particle-mesh Ewald (SPME) method[75,58] and the long-range cutoff of 50 Å which was always larger than the system size. The van der Waals and SPME direct sum interactions were truncated at 9 Å with the value of Ewald parameter $\beta \approx 0.35$.

The initial state for B → A transitions was prepared as before[58] with the canonical B-DNA[76] used a standard conformation. The DNA molecule was first immersed in a large rectangular TIP3P[77] water box, and next, external solvent molecules were removed by using a spherical distance cutoff from DNA atoms. The cutoff radius was adjusted to obtain the desired number of water molecules remaining. The drop was neutralized by randomly adding the necessary number of Na^+ ions. Simulations of A → B transitions started from the final structure of a B → A transition obtained with the lowest hydration.

Every system was energy minimized first with the solute held rigid and then with all degrees of freedom. Dynamics were initiated with the Maxwell distribution of generalized momenta at 250 K and equilibrated at this temperature during several picoseconds. Production trajectories were computed with the temperature bound to 300 K by the Berendsen algorithm[78] with a relaxation time of 10 ps. For better comparison with earlier simulations of A ↔ B transitions, the original Cornell et al. force field[66] was used. Trial simulations carried out with other versions of the AMBER force filed[79,80] suggest, however, that the main conclusions of this study are not force field dependent. Duration of production runs varied from 5 to 25 ns depending upon the observed character of dynamics. The conformations were saved with a 2.5 ps interval. Programs Curves,[81] XmMol,[82] and Mathematica by Wolfram Research Inc. were employed in the data processing.

Results and Discussion

An example of the molecular transformation we study is shown in Figure 1. The top row exhibits the canonical B- and A-DNA structures. The process begins with plate 1 where we see a snapshot of the first saved state during a production run started from the canonical B-DNA conformation. This system involves a dodecamer DNA fragment with 22 Na^+ and 400 water molecules. It is seen that after the equilibration some ions have already entered the major groove while a thin water shell covers the surface of the DNA molecule. One may notice also a small narrowing in the middle of the minor groove which is a well-known distinctive feature of the crystal structure of this dodecamer. This initial trend is only temporary, however. The number of water molecules in the system is about 17 per nucleotide, which is less than the limiting hydration number

(59) Seibel, G. L.; Singh, U. C.; Kollman, P. A. *Proc. Natl. Acad. Sci. U.S.A.* **1985**, *82*, 6537−5640.
(60) Miaskiewicz, K.; Osman, R.; Weinstein, H. *J. Am. Chem. Soc.* **1993**, *115*, 1526−1537.
(61) Norberg, J.; Nilsson, L. *Proc. Natl. Acad. Sci. U.S.A.* **1996**, *93*, 10173−10176.
(62) Brünger, A.; Brooks, C. L., III; Karplus, M. *Chem. Phys. Lett.* **1984**, *105*, 495−500.
(63) Belch, A. C.; Berkowitz, M. *Chem. Phys. Lett.* **1985**, *113*, 278−282.
(64) Warshel, A.; King, G. *Chem. Phys. Lett.* **1985**, *121*, 124−129.
(65) Wing, R.; Drew, H.; Takano, T.; Broka, C.; Tanaka, S.; Itakura, K.; Dickerson, R. E. *Nature* **1980**, *287*, 755−758.
(66) Cornell, W. D.; Cieplak, P.; Bayly, C. I.; Gould, I. R.; Merz, K. M.; Ferguson, D. M.; Spellmeyer, D. C.; Fox, T.; Caldwell, J. W.; Kollman, P. A. *J. Am. Chem. Soc.* **1995**, *117*, 5179−5197.
(67) Young, M. A.; Ravishanker, G.; Beveridge, D. L. *Biophys. J.* **1997**, *73*, 2313−2336.
(68) Duan, Y.; Wlkosz, P.; Crowley, M.; Rosenberg, J. M. *J. Mol. Biol.* **1997**, *272*, 552−572.
(69) Mazur, A. K. *J. Comput. Chem.* **1997**, *18*, 1354−1364.
(70) Mazur, A. K. In *Computational Biochemistry and Biophysics*; Becker, O. M., MacKerell, A. D., Jr., Roux, B., Watanabe, M., Ed.; Marcel Dekker: New York, 2001; pp 115−131.
(71) Mazur, A. K. *J. Am. Chem. Soc.* **1998**, *120*, 10928−10937.
(72) Mazur, A. K. *J. Chem. Phys.* **1999**, *111*, 1407−1414.
(73) Mazur, A. K. *J. Phys. Chem. B* **1998**, *102*, 473−479.
(74) Mazur, A. K.; Sumpter, B. G.; Noid, D. W. *Comput. Theor. Polym. Sci.* **2001**, *11*, 35−47.
(75) Essmann, U.; Perera, L.; Berkowitz, M. L.; Darden, T.; Lee, H.; Pedersen, L. G. *J. Chem. Phys.* **1995**, *103*, 8577−8593.
(76) Arnott, S.; Hukins, D. W. L. *Biochem. Biophys. Res. Commun.* **1972**, *47*, 1504−1509.
(77) Jorgensen, W. L.; Chandreskhar, J.; Madura, J. D.; Impey, R. W.; Klein, M. L. *J. Chem. Phys* **1983**, *79*, 926−935.
(78) Berendsen, H. J. C.; Postma, J. P. M.; van Gunsteren, W. F.; DiNola, A.; Haak, J. R. *J. Chem. Phys.* **1984**, *81*, 3684−3690.
(79) Cheatham, T. E., III; Cieplak, P.; Kollman, P. A. *J. Biomol. Struct. Dyn.* **1999**, *16*, 845−862.
(80) Wang, J.; Cieplak, P.; Kollman, P. A. *J. Comput. Chem.* **2000**, *21*, 1049−1074.
(81) Lavery, R.; Sklenar, H. *J. Biomol. Struct. Dyn.* **1988**, *6*, 63−91.
(82) Tuffery, P. *J. Mol. Graphics* **1995**, *13*, 67−72.

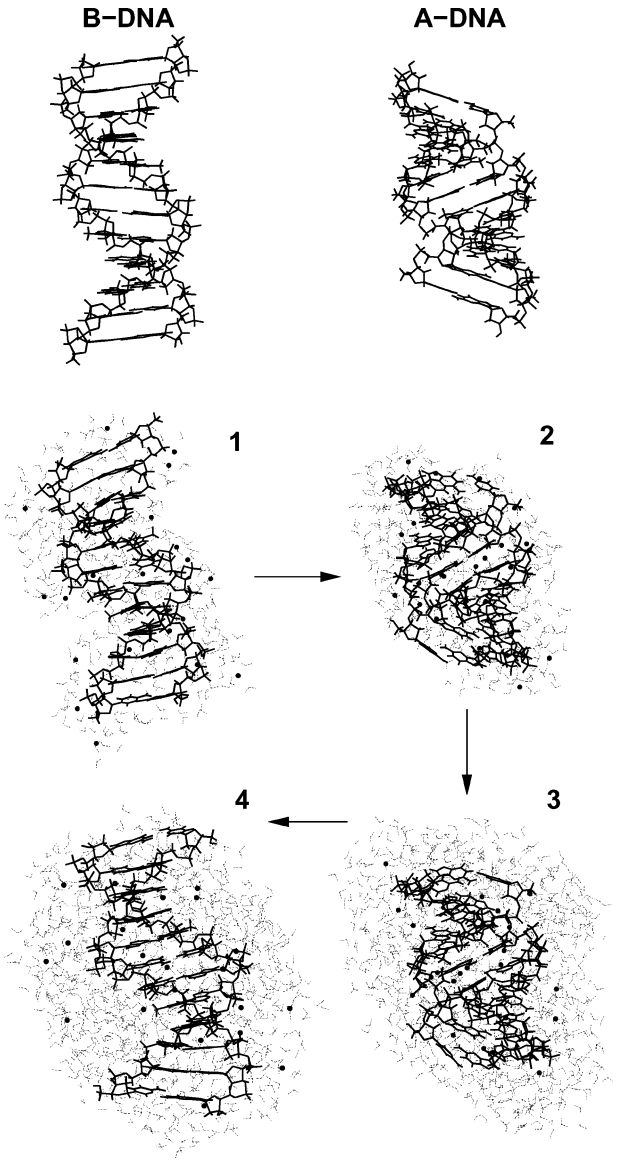

Figure 1. An example of a reversible B → A transition. Water molecules and Na^+ ion positions are shown by broken lines and large dots, respectively.

for B-DNA.[3,83] In dynamics, it looks as if water tries to form a smooth spherical drop around the DNA fragment, and this is achieved owing to a B → A transition. Plate 2 shows a snapshot after 2 ns of dynamics. It is seen that the DNA molecule went to the characteristic A-form conformation with a wide minor and narrow major grooves. Note that a substantial part of the Na^+ ions is sandwiched in the major groove between the two opposite sugar−phosphate strands. The more compact A-form structure allows water to form a nearly spherical drop that covers the DNA fragment. After the transition, the structure remains stable during the time accessible in calculations.

The final state of the previous trajectory was used as a starting point for the second run to obtain an inverse A → B transition. For this purpose, the system was surrounded by 600 additional water molecules to increase their number to 1000. Plate 3 in Figure 1 displays a snapshot from the beginning of the second production run. Now the number of water molecules is about 42 per nucleotide, which corresponds to B-DNA hydration numbers. The last plate in Figure 1 shows a snapshot after 2 ns of dynamics. As we see, the DNA molecule really went back from the A- to B-DNA conformation and the narrowing in the middle of the minor groove reappeared.

(83) B-DNA is generally known to become unstable with respect to A-DNA and C-DNA for hydration numbers Γ below 20 molecules per nucleotide.[3] The midway transition point can be estimated as Γ ≈ 15.[3,96] The limiting Γ values, that is, hydration degrees beyond which the DNA properties do not change, are around 36 and 5 for B-DNA and A-DNA, respectively.[97,98] In solution, the midway points of B ↔ A transitions for isolated DNA fragments vary with their size and sequence.[5,26]

Table 1. Some Structural Parameters of DNA Conformations after Either A → B or B → A Transition Obtained in Dynamics[a]

size	transition	rmsd-A	rmsd-B	Xdisp	inc	twist	rise	time
400(16.7)	B → A	2.1	6.5	−4.3	23.9	33.6	2.3	1.5
500(20.8)	B → A	1.8	6.4	−4.2	21.7	32.2	2.4	18.0
600(25.0)	B → A	1.8	6.1	−4.2	20.4	32.0	2.5	20.0
800(33.3)	A → B	3.3	3.4	−2.9	10.7	32.7	3.1	5.0
1000(41.7)	A → B	3.3	3.4	−3.2	9.2	31.4	3.1	1.0
2000(83.3)	A → B	3.5	3.8	−3.5	8.2	30.6	3.2	1.5

[a] The drop size is given as the number of water molecules, with their number per nucleotide in parentheses. The rmsd from the canonical A- and B-DNA and sequence averaged helical parameters are shown for conformations averaged over the last nanosecond of dynamics. The helical parameters are measured for the six central base pairs with respect to the global helical axis as computed by Curves.[81] All distances are in angströms, and angles, in degrees. The approximate time of transition (in nanoseconds) corresponds to the end of the sugar switch phase.

The sequence of transitions shown in Figure 1 suggests that there exists a critical level of hydration characterized by an equal probability of A- and B-forms, if the transition is cooperative or, by some structures, intermediate between the two. To gain a rough estimate of this midway point, a series of MD simulations was carried out with the size of the water drop systematically varied. The results obtained are summarized in Table 1. The corresponding trajectories were started from standard A-DNA and B-DNA states and continued as long as necessary to reach either an A → B or a B → A transition. In all cases, either no transition or a transition in one direction only was obtained. For intermediate hydration values, notably, for 21 and 25 water molecules per nucleotide, very long trajectories were necessary. After the A → B transitions, dynamics usually sampled conformations intermediate between the two forms and the average structural parameters established very slowly. In addition, it is known that the Cornell et al. force field systematically underestimates the helical twist in B-DNA.[79] These two factors together explain a noticeable deviation of the final B-DNA parameters in Table 1 from the canonical values. The results summarized in Table 1 suggest that the hydration of 25 water molecules per nucleotide can serve as a rough estimate of the transition point. This value is somewhat higher but rather close to the well-known experimental estimates,[3,83] which is very encouraging taking into account the large number of experimental and computational parameters involved in such comparisons.

As seen in Figure 1 and Table 1, the A-DNA structure obtained in dynamics under minimal hydration is more compact and slightly overwound with respect to the canonical conformation. The width of its major groove averaged over the last nanosecond is about 2 Å below the canonical value. At higher hydration, the A-DNA states had slightly wider major grooves, with the helical parameters closer to the canonical A-DNA values (see Table 1). In all cases, however, structures with the major groove width similar to that in the canonical A-DNA were observed only temporarily in intermediate transition phases, and

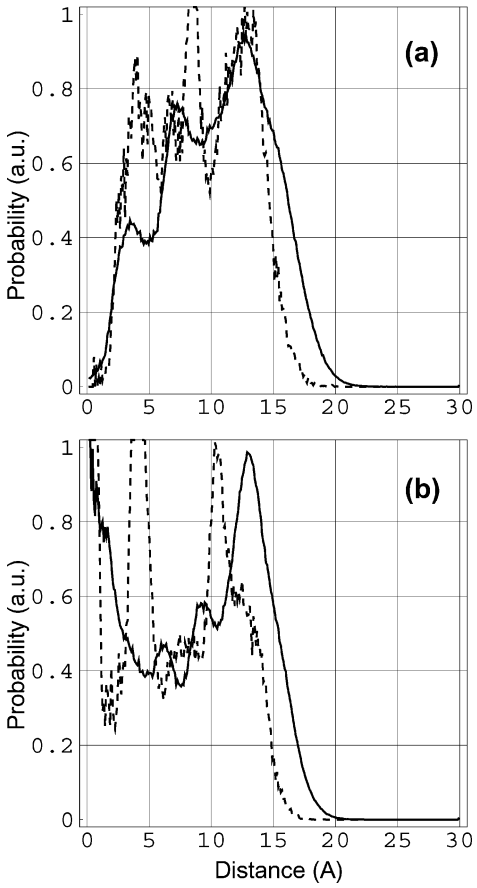

Figure 2. Characteristic cylindrical radial distribution functions for water oxygens (solid lines) and Na^+ ions (dashed lines) for B-DNA (a) and A-DNA (b) states. DNA structures saved in dynamics together with surrounding water and counterions were superimposed with either B-DNA (a) or A-DNA (b) canonical forms with the global coordinate OZ direction as the common helical axis. The corresponding DNA helical diameter is approximately 10 Å in both plates. The Na^+ ions and water oxygens were counted in coaxial 0.1 Å thick cylinders. The distributions are volume normalized, that is, scaled with a factor of $1/r$. No smoothing was applied. The final plots were area normalized.

they seemed to be unstable with respect to the more compact conformation shown in plate 2 of Figure 1. Visual inspection reveals that in such structures the phosphate groups opposed across the major groove are similarly close or even closer to each other than the neighboring phosphates in the same strand. They are linked by multiple water bridges, and at least one such bridge is usually replaced by a Na^+ ion slightly shifted either inside or outside the helix. With intermediate hydration numbers, however, this pattern was less clear, with both Na^+ and the opposite phosphate groups often hydrated separately.

The spatial distributions of water and ions around DNA after B → A and A → B transitions are compared in Figure 2. The data for Figure 2a were collected in the course of the fourth trajectory mentioned in Table 1 during a 4.5 ns period after the A → B transition. The results in Figure 2b were obtained in a trajectory alternative to the third one mentioned in Table 1, that is starting from A-DNA, which sampled only A-states. These two model systems correspond to hydration numbers closest to the critical value from the B- and A-DNA sides, respectively. They are rather similar in size; nevertheless, the corresponding distributions are strongly different. For the B-DNA state in Figure 2a, we have a pattern encountered earlier.[58] The water oxygen distribution shows the relative accessibility of the space available for counterions. Its three peaks seen in Figure 2 are due to the first major groove water layer, the other layers in both grooves, and the remaining outer shell, respectively.[58] The Na^+ distribution suggests that ions occupy the same space but prefer to enter the DNA grooves rather than stay outside. Compared to earlier simulations in a larger drop,[58] here the outer Na^+ shell is reduced, with excess ions entering the DNA diameter and additional peaks emerging in the internal part of the distribution.

A similar analysis of Figure 2b reveals a few instructive features. First, it is seen that the center of the helix is accessible to water and ions. Compared to Figure 2a, a relatively large fraction of water remains outside the helical diameter, but it is almost void of ions. At the same time, within the helical diameter, there are two prominent Na^+ peaks that do not correspond to the available space, suggesting that ions are kept here by strong interactions. The peak at around 4 Å can be attributed to Na^+/base contacts of which binding to N7 atoms of purines is the most common. The peak at around 10 Å corresponds to interactions with phosphates in the opening of the major groove, and it is seen that this peak accounts for the largest fraction of Na^+ ions.

One of the trajectories mentioned in Table 1 is detailed in Figure 3. This simulation started from the canonical B-DNA with a water shell of 500 molecules (20.8 per nucleotide). Some of the parameters used for the plots in Figure 3 deserve preliminary comments, notably, the backbone length and the width of the two grooves. The backbone length is computed as the average distance between the centers of consecutive sugar rings. Note that its value is larger in A-DNA than in B-DNA in contrast to the inter-phosphate distance which is smaller.[3] In fact, in a B → A transition, the sugars are moved to the outer surface of the double helix, with the helical diameter of the sugar trace increased by nearly 6 Å, which is one of the most remarkable internal moves involved in the transition.

Measuring DNA grooves in the course of dynamics is not trivial because the corresponding distances cannot be taken between fixed atoms. For instance, if the A-DNA major groove is measured as the shortest inter-phosphate separation, for a given phosphorus atom of the "Watson" strand we should take that from the "Crick" strand shifted by 8 base pairs. In B-DNA, however, the line joining these two atoms would be almost parallel to the helical axis, whereas the most appropriate partner is shifted by 3 or 4 base pairs only. In the procedure used here, the grooves are evaluated by perpendicular cross-sections of spatial traces of C5′ atoms.[84] For each line between consecutive C5′ atoms of the "Watson" strand, the distance is measured from an appropriate C5′ atom of the "Crick" strand and the result is assigned to the corresponding residue of the "Watson" strand. In addition, for each C5′ atom of the "Watson" strand, the distance is measured from an appropriate line joining two consecutive C5′ atoms of the "Crick" strand, and this latter distance is assigned to the middle point between the corresponding two residues of the "Watson" strand. This method produces smooth profiles that serve for the surface plots shown in plates (b) and (c). Near the helical termini, however, the perpendicular cross-sections intersect only one of the two backbone strands. As a result, in the dodecamer A- and B-DNA, the major groove is defined for residues 1, ..., 5 and 1, ..., 9,

(84) Mazur, A. K. *J. Mol. Biol.* **1999**, *290*, 373−377.

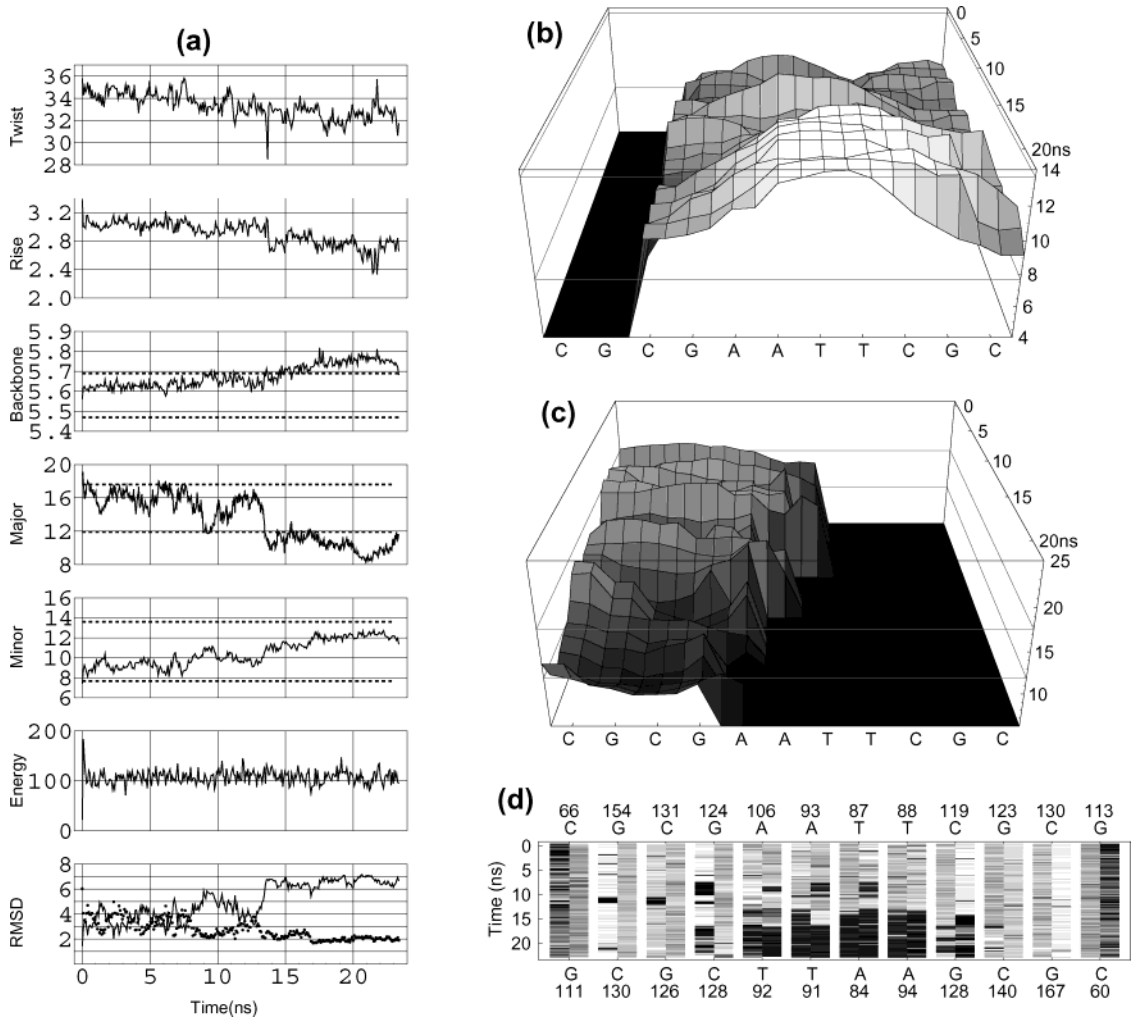

Figure 3. A representative example of the dynamics of a B → A transition. (a) Time traces of some important parameters. From top to bottom: the average twist and rise with respect to the global helical axis; the average backbone length computed as the distance between the centers of consecutive sugar rings; the average width of the major and minor grooves; the total energy; the rmsd from the canonical A-DNA (dotted line) and B-DNA (solid line). The horizontal broken lines in some frames mark the canonical B- and A-DNA values. (b) The time evolution of the minor groove profile. The surface is formed by 23 minor groove profiles equally spaced in time and each averaged over a 75 ps interval. The profile on the front face corresponds to the final DNA conformation. The groove width is evaluated by perpendicular cross-sections of space traces of C5′ atoms,[84] with the measured distances assigned to the sequence of the upper ("Watson") strand. The empty zone on the left corresponds to the region where the groove could not be measured. The width is given in angstroms and the corresponding canonical A- and B-DNA levels are marked in all plates by the thin straight lines. (c) The time evolution of the major groove profile. The surface is constructed similarly to plate (b). The empty zone on the right corresponds to the region where the groove could not be measured. (d) Dynamics of sugar pucker pseudorotation. The pucker phases observed in dynamics were reduced to the (0°, 180°) interval by replacing the rare outer phases with the closest of the two boundary values. The minimal and the maximal phases obtained were assigned the black and the white colors, respectively, with intermediate values mapped linearly to the gray scale levels. Each base pair step is characterized by a column consisting of two subcolumns, with the left subcolumns referring to the sequence written above in the 5′−3′ direction from left to right with the time averaged phases given on top. The right subcolumns refer to the complementary sequence shown below together with the corresponding time averaged phases.

respectively; that is, it shortens considerably in the course of the B → A transition. A similar, but smaller effect exists for the minor groove as well. These features are clear in plates (b) and (c) of Figure 3. The average widths were computed for the zones where the corresponding grooves were defined at a given moment.

The B → A transition seen in Figure 3 is relatively slow, with the final structure established only after 18 ns. An early B → A transition occurred close to one of the termini at around 10 ns. However, it was incomplete and inverted 2 ns later. According to the two rmsd traces, the final transition started at 13 ns. Until that, the dynamics sampled midway conformations between A- and B-forms, which is not that far from normal B-DNA dynamics with the same potentials.[53,67,68] It may be seen that the minor groove profile periodically switched from narrowing to widening in the middle. At about 13 ns, the two rmsd traces drastically moved close to their final levels. Simultaneously, the major groove width fell by almost 10 Å and went below the A-DNA level. At that time, the molecule already looked very much like A-DNA, with the instantaneous rmsd-A values around 2 Å, but almost all sugars still had their puckers in the south region. The final phase of the transition is slower, and during this phase, the sugars in the middle AATT tetraplet switch to the north. In this middle zone, the transition to the A-form is complete, whereas the three terminal base pairs remain in an intermediate conformation with south sugar puckers. The zone of the B → A transition is determined by its middle position in the DNA fragment rather than by its sequence, which is A-phobic.[26] In other words, in this case, the

B-philicity of DNA ends[85] appears to be stronger than the sequence preferences. At the same time, in other simulations, we observed that fragments with GC-rich A-philic cores go to A-form much easier; that is, this model system is also able to reproduce sequence dependence of the B ↔ A transitions. Such effects as well as force field dependent aspects of these simulations will be discussed elsewhere.

Although the structural parameters shown in plate (a) differ by the amplitudes of fluctuations, they all reveal a slow overall drift suggesting a downhill motion of the system on a free energy surface. In contrast, the total energy remains stable throughout the trajectory except the initial phase. This means that, already during heating, the system finds a balance of internal interactions maintained afterward, and consequently, the observed steady downhill character of the transition has an entropic origin. The precise nature of this entropic force is not clear. The backward A → B transitions have qualitatively similar kinetics suggesting that this feature is not due to the properties of the A- and B-DNA forms but results from the specific setup of simulations.

In the backward A → B transitions, the sequence of events is inverted; that is, the sugar puckers quickly switch to the south, whereas the rmsd's and the groove widths need sometimes many nanoseconds to reach stationary B-DNA values. This order of events does not depend on the amount of water added, and it is slower than in earlier reported AMBER simulations.[51,54] The apparent reason is that during the B → A transition a large number of metal ions enter the major groove when it is still wide. A high ion concentration in the major groove is one of the factors that supposedly stabilize the A-DNA conformation.[31,32] In contrast, when the trajectory is to be started from the canonical A-DNA, the major groove is narrow from the beginning, and a very long equilibration period should be necessary for the same number of ions to reach optimal positions.

The possibility of B ↔ A transitions in longer and shorter DNA fragments has been checked in a series of simulations summarized in Figure 4. The foregoing results suggested that the B → A transitions in a water drop are mainly driven by electrostatic interactions between counterions and backbone phosphates across the major groove. A characteristic A-form major groove can be formed starting from eight base pairs, and as seen in Figure 3c, its length in a dodecamer A-DNA is between four and five nucleotides. One could expect, therefore, that B → A transitions would progressively become more difficult as the DNA is shortened. All trajectories shown in Figure 4 started from B-DNA with the lowest degree of hydration used in Table 1. The number of Na^+ and the size of the water drop were changed according to the DNA chain length. As expected, relatively rapid B → A transitions are observed in the original dodecamer and its longer derivatives. In contrast, the transition did not occur in shorter fragments. The hexamer always remained in a B-DNA conformation with the average rise and inclination around 3.45 Å and −2.5 °, respectively, indicating that the structure deviated from the canonical B-DNA but not toward the A-form. The octamer and decamer fragments exhibited dynamics somewhat similar to that of the dodecamer, with accumulation of Na^+ ions in the major groove and noticeable compression of the DNA structure; however, the

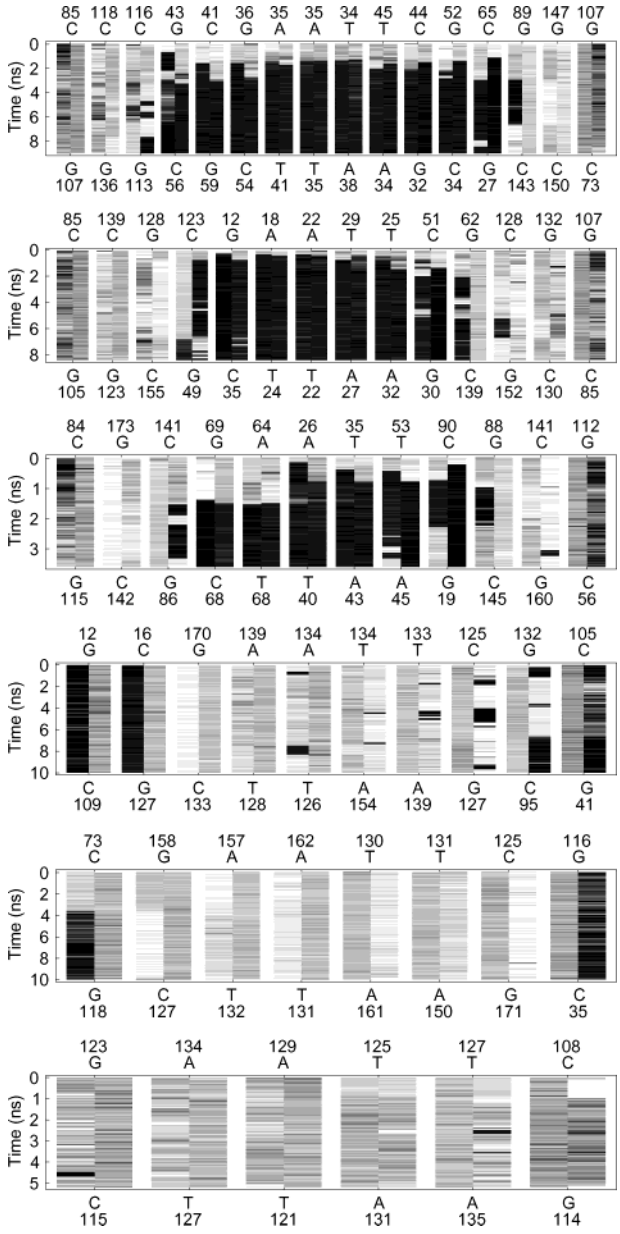

Figure 4. Dynamics of B → A transitions in DNA fragments obtained by elongation and truncation of the initial sequence. For details, see the legend to plate (d) of Figure 3.

B → A transition did not occur. Moreover, one of the terminal base pairs in the decamer was broken, with water bridges formed between the two nucleotides, which apparently helped to move closer the opposite phosphate strands in the major groove. This effect was reproduced in a repeated run with hydrogen bonds in terminal base pairs enforced by weak additional restraints. The last observation suggested that the three shorter fragments in Figure 4 would not go to A-form even in much longer dynamics.

Based upon the described qualitative character of DNA dynamics, one can consider two main physical factors as the possible driving forces of the B ↔ A transition under low hydration. First, water tends to reduce its contact surface with vacuum and forms a spherical drop forcing the DNA fragment to shrink. This force can be considered as surface tension or as a particular case of the hydrophobic effect, with a vacuum in place of a nonpolar solvent. The second factor is the increased

(85) Minchenkova, L. E.; Schyolkina, A. K.; Chernov, B. K.; Ivanov, V. I. *J. Biomol. Struct. Dyn.* **1986**, *4*, 463−476.

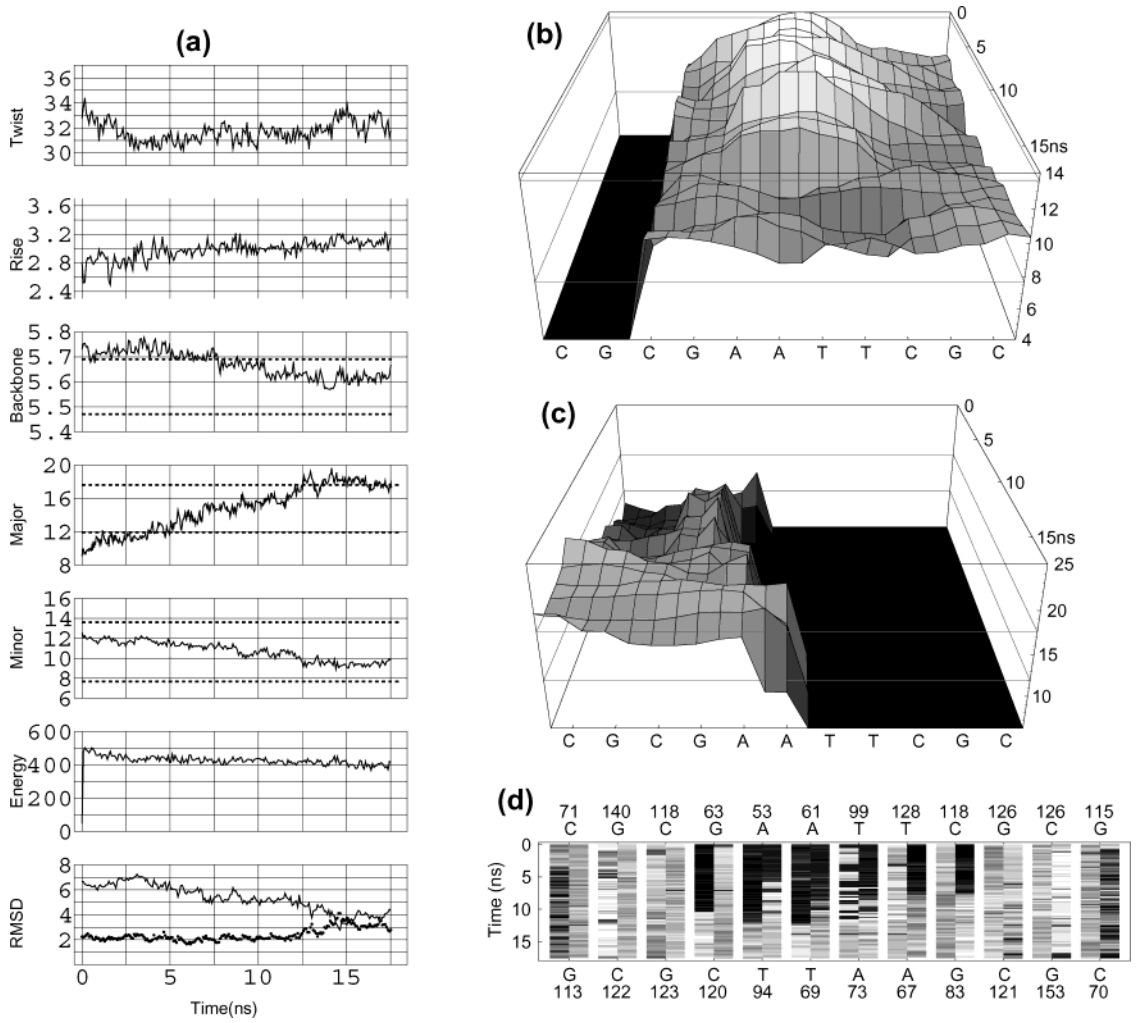

Figure 5. A dynamics of an A → B transition in a 600 water molecule drop with increased NaCl concentration. For details, see the legend to Figure 3.

concentration of Na^+ ions. These two alternatives were checked in additional simulations under modified conditions. To check separately the role of the surface tension, the DNA fragment was neutralized by reducing the partial charges of OP atoms, and two 10 ns dynamics were run starting from the canonical B-DNA under the lowest and the highest hydration without counterions in the water drop. These two trajectories turned out to be rather similar. The sampled conformations clearly belonged to the B-DNA family, but they were slightly underwound with respect to the usual structures computed under optimal conditions with explicit counterions. Under the low hydration, the duplex looked slightly compressed, with a subtle shift of the average helical parameters toward the A-form values, but all sugar puckers remained at the south and the grooves had usual B-DNA shapes.

The effect of the increased concentration of Na^+ ions near the double helix can also be 2-fold. On one hand, this should reduce the water activity and stimulate more economical hydration patterns of phosphate groups as in the well-known mechanism of B → A transitions.[29] At the same time, the counterion cloud can affect the DNA structure directly by the medium and long-range electrostatic interactions. The role of the water activity was checked in two simulations with added NaCl. Earlier it was reported that high NaCl does not cause B → A transitions in conventional simulations with periodical boundaries.[32] To make a more stringent test, here the NaCl concentration was increased under the midway hydration as estimated in Table 1. It was hoped that under such conditions an increased salt concentration can produce a clear qualitative effect upon the dynamics. The initial A- and B-DNA states in a water shell of 600 molecules were modified by replacing 66 randomly chosen water molecules with 33 Na^+ and 33 Cl^- ions. After that, 66 water molecules were added to maintain the earlier hydration level. The effective concentration of Na^+ was thus raised from 2 M to 5 M. The two systems were re-equilibrated with the standard protocol, and long trajectories were computed to obtain either an A → B or a B → A transition. In contrast to the tests in Table 1, here an A → B transition was obtained after about 13 ns of dynamics as shown in Figure 5. The dynamics exhibited in this figure is typical of the A → B transitions described above, although its kinetics are much slower than those in Table 1. Note, for instance, that the average twist first decreases and then slowly goes up. This behavior is due to the compact overwound starting A-DNA conformation corresponding to the lowest hydration in Table 1. The initial decrease of the average twist occurs in the A-DNA phase, with the structure passing close to the canonical A-form. The complementary B-DNA trajectory was similar in duration, and it showed no trend toward A-form.

In the animations of these trajectories, progressive crystallization of NaCl was seen, with large blocks of typical cubic NaCl lattice found in the major DNA groove in the end of both

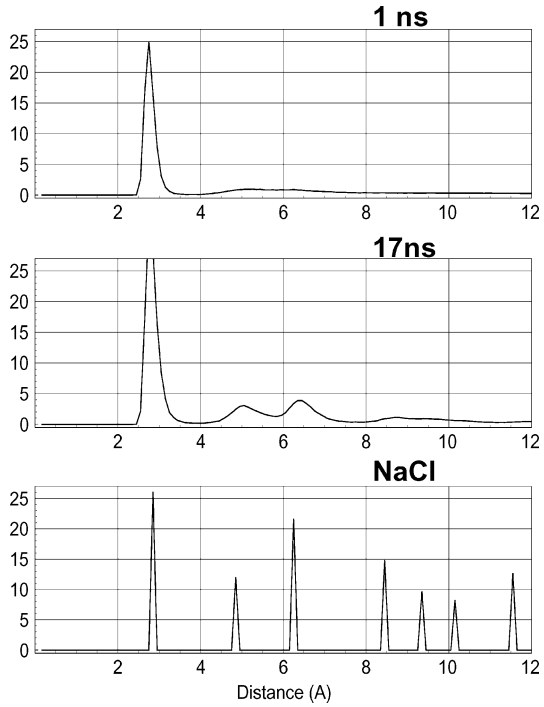

Figure 6. Na···Cl radial distribution functions (rdf) evaluated for the 1st (top) and the 17th (middle) nanoseconds of dynamics in Figure 5. The rdf's are normalized assuming 5 M bulk NaCl concentration. The corresponding rdf computed for an inifinite NaCl cubic lattice is shown in the bottom plate.

trajectories. This effect can be seen in Figure 6. The radial distribution functions were computed by taking into account all Na−Cl pairs in the water drop configurations saved during the first and the last nanoseconds of dynamics. The distributions were arbitrarily normalized assuming a 5 M "bulk" NaCl concentration. The bottom distribution was computed for an infinite cubic lattice corresponding to the Na−Cl equilibrium distance of 2.81 Å. Note that during the first nanosecond, almost all Cl^- ions were already paired with Na^+, but no long-range structure can be distinguished. At the end of dynamics, however, the peaks at around 5 and 7 Å characteristic of the cubic packing are clearly seen and unresolved longer range peaks are also distinguishable.

Addition of NaCl is supposed to stimulate A → B transitions in fiber DNA crystals.[86] Moreover, NaCl crystallization occurs in DNA fibers at 75% relative humidity if the salt content is above 6 of the DNA weight,[86] which gives a 4.8 M effective concentration of NaCl according to the reported water/DNA adsorption curves.[87] One may note, therefore, that the overall effect of the added salt in our simulations qualitatively agrees with experiments. The observed shift toward the B-form may be caused by the NaCl crystallization either directly, by forcing the major groove to open, or indirectly, by pushing water out from the major groove together with some free Na^+ ions. In any case, however, these results suggest that it is not the water activity reduced by ions that causes the B → A transitions in small drops. Instead, this unexpected effect reveals the possibility of a paradoxical inverse interpretation. In fact, it is the DNA molecule itself that strongly reduces the activity of surrounding water and enforces crystallization of NaCl.

The last simulations suggest that B → A transitions in small water drops are induced by a united effect of the limited water shell and counterions and not by one of these factors considered separately. A simple and attractive mechanism that accounts for all the above results is as follows. The B → A transition is caused by direct electrostatic interactions between mobile metal cations and phosphate groups in the opening of the major DNA groove. When the local cation concentration exceeds a certain critical value, the inter-phosphate repulsion is inverted to attraction. A similar idea is long discussed in the context of DNA bending,[88−90] and it was earlier proposed by Cheatham and Kollman as one of the possible mechanisms responsible for stability of the A-form.[31,32] The strong inter-phosphate attraction immediately results in local DNA bending and, eventually, in a B → A transition at the opposite side of the double helix. When the length of the major groove exceeds one helical turn, the apparent bend becomes uniform shrinking. The role of the limited water shell consists in pushing the counterion cloud surrounding DNA inside the diameter of the double helix. The counterions avoid loosing their hydration shells and are forced to come closer to DNA. The surface tension at the drop boundary plays a certain role, but it is the reduced overall space available for counterions that seems more important. This simple model explains well our results, and below, we consider why and how it may work in other conditions as well.

Concluding Discussion

Clarification of the detailed mechanisms involved in the DNA polymorphism is an important challenge for rapidly progressing computational methods in molecular biophysics.[91] Here, for the first time, reversible B ↔ A transitions were obtained *in silico* in a simulated titration experiment by smooth variation of water content. The environment conditions used were not earlier encountered in experiments; nevertheless, the qualitative features found seem credible and likely to exist in analogous experimental conditions. First, the computed pattern of DNA transformations is physically sensible and agrees with known experimental trends, notably, as regards the principal effect of the amount of bound water. Second, these calculations give the most accurate currently possible prediction of the true properties of DNA fragments in small water drops. Really, the Cornell et al. force field[66] was earlier shown to produce DNA dynamics in good agreement with experiments.[91] Its parameters were fitted with small molecule data only, and they were never specifically adjusted for periodical boundary conditions. In our case, no artificial interactions are introduced, while those between periodical images are eliminated.[58] There are all reasons to believe, therefore, that our simulations reproduce correctly the dynamics of DNA transformations in such unusual conditions.

Qualitatively, the results obtained here agree with earlier studies. Cheatham and Kollman were the first to obtain an A → B transformation in pure water and stable A-DNA dynamics in 85% EtOH.[51,31] Visual inspection of the reported A-DNA snapshots[31] shows that our structures are quite similar to those

(86) Cooper, P. J.; Hamilton, L. D. *J. Mol. Biol.* **1966**, *16*, 562−563.
(87) Falk, M.; Hartman, K. A., Jr.; Lord, R. C. *J. Am. Chem. Soc.* **1962**, *84*, 3843−3846.
(88) Mirzabekov, A. D.; Rich, A. *Proc. Natl. Acad. Sci. U.S.A.* **1979**, *76*, 1118−1121.
(89) Levene, S. D.; Wu, H.-M.; Crothers, D. M. *Biochemistry* **1986**, *25*, 3988−3995.
(90) Rouzina, I.; Bloomfield, V. A. *Biophys. J.* **1998**, *74*, 3152−3164.
(91) Cheatham, T. E., III.; Kollman, P. A. *Annu. Rev. Phys. Chem.* **2000**, *51*, 435−471.

in EtOH as regards the width of the major groove, preferred positions of Na^+ ions, and a B-like character of the DNA termini, which gives the molecule a strong apparent bend to the major groove. Moreover, the reported stabilization of A-DNA in EtOH[31] required that the molecule was first covered by water and then by EtOH as an outer shell. The necessity of such double phase hydration was confirmed by Sprous et al.[54] Although water and EtOH could mix in dynamics, it seems evident that, to be stable in simulations, the A-form should be contained in a small water shell. Cheatham and Kollman showed also that a B → A transition can be provoked by placing polycationic ligands to the major groove between the opposite phosphate strands.[32] Our results confirm that the accumulation of positively charged counterions in the major groove of B-DNA is, perhaps, the major driving force of this transition.

Although one cannot exclude that the A ↔ B transitions in different conditions are due to radically different mechanisms, it is tempting to consider the possibility that the electrostatic model outlined above in fact operates in all such cases. This model is readily transferable from water drop to DNA in fibers under different relative humidities. The too narrow major groove of the computed A-DNA, in fact, is not a dramatic discrepancy. The major groove in the A-DNA conformations available in NDB[92] varies so strongly that this parameter can hardly be considered as a well-defined attribute of the A-form. It is possible also that the parametrization of Na^+ ions in the Cornell et al. force field[66] underestimates its binding to water with respect to negatively charged atoms. In our dynamics, correct canonical major groove width was observed during transitions as long as Na^+ ions kept their first hydration shells and avoided direct contacts with the phosphate groups.

Another defect of the computed A-DNA consists of the strong B-philicity of the termini accompanied by bending to the major groove. These two features are mutually related because the double helix is long known to bend at an A/B boundary.[93] This defect, however, is only apparent because it qualitatively agrees with experimental data. The B-philicity of DNA ends has to be assumed when A ↔ B transitions in solution are considered.[85] Moreover, many single crystal A-DNA structures appear to smoothly bend to the major groove when analyzed with the Curves program,[81] with this trend being particularly evident for complete helical turns.[44,94,95] In our simulations, these features are just accentuated due to the excessively narrow major groove, which requires stronger bending, and also because our sequences are not A-philic as in all single crystal A-DNA fragments.

The solution A ↔ B transitions caused by nonpolar organic solvents can also be interpreted in terms of the above electrostatic model. For this purpose, it is sufficient to consider what would happen if our water drops were put in EtOH, for instance. The water activity inside the drop is strongly reduced by DNA itself and its counterion shell. In infinite water, the activity coefficient grows with the distance from DNA. It is perhaps close to zero near the double helix and approaches to one outside the counterion cloud, that is, beyond 10 Å from DNA. EtOH is easily miscible with normal water but not with the low activity water near DNA. This argument can be illustrated by the above-discussed crystallization of NaCl in the DNA environment at concentrations much below its standard solubility limit. The water molecules would leave the drop and go to EtOH until the outer water activity becomes equal to that inside the drop. In other words, the water activity in the added nonpolar phase determines the size of the drop and, consequently, the state of the A ↔ B equilibrium. That is why B ↔ A transition curves in different solvents converge when water activity is used as a parameter.[34] More polar solvents such as MetOH and ethylene glycol do not cause B → A transitions possibly because they solvate counterions rather than push them inside the double helix.

Both the apparent B-philicity of the DNA ends and the chain length dependence of the B → A transitions observed in our simulations agree with experiments in solution.[16,17,85] Another salient feature nicely reproduced is the cooperative character of the transition, with the minimal length of the cooperative fragment of around one helical turn. This cooperativity is not caused by the sugar pseudorotation barrier because during B → A transitions the sugars switch last. Instead it is conditioned by the A-DNA geometry and the character of the electrostatic interactions in the major groove. In A-DNA, the first phosphate in the "Watson" strand is close to the "Crick" phosphate of the $(n + 8)$th base pair. Suppose the B → A transition is enforced by the counterion-mediated electrostatic attraction between these groups. In this case, the eight intermediate base pairs form the DNA fragment that should be bent or compressed in order that these two phosphates could come close to each other. The positive energy of this mechanical deformation should be compensated by the negative electrostatic energy of solvent cations sandwiched between the phosphates. One step of such "electrostatic sandwich" is probably insufficient, and octamer DNA double helices should not generally go to the A-form. In a nanomer A-DNA, however, the sandwich length is increased by one step while the deformation energy is increased only by a fraction of the initial gap. Therefore, the energetic balance is progressively shifted in favor of the A-form as the chain length is increased. In long DNA, the boundary between the A- and B-forms has an excess energy because the energy gap of the initial octamer remains effectively shared between the two opposite boundaries. The foregoing qualitative pattern exactly corresponds to the one-dimensional Ising model of cooperative transitions.[15]

As we see, one cannot exclude that this electrostatic model, originally proposed by Cheatham and Kollman,[31,32] is, in fact, the general mechanism of A ↔ B transitions in DNA. The above problems are certainly far from being clear, and many related issues should be addressed in future simulation and experimental studies. For instance, this model should explain the inability of Li^+ ions to induce the B → A transitions, perhaps assuming that the large size of their hydration shells does not allow them to accumulate to high enough concentrations in the limited space

(92) Berman, H. M.; Olson, W. K.; Beveridge, D. L.; Westbrook, J.; Gelbin, A.; Demeny, T.; Hsieh, S. H.; Srinivasan, A. R.; Schneider, B. *Biophys. J.* **1992**, *63*, 751−159.
(93) Selsing, E.; Wells, R. D.; Alden, C. J.; Arnott, S. *J. Biol. Chem.* **1979**, *254*, 5417−5422.
(94) Verdaguer, N.; Aymami, J.; Fernandez-Forner, D.; Fita, I.; Coll, M.; Huynh-Dinh, T.; Ingolen, J.; Subirana, J. A. *J. Mol. Biol.* **1991**, *221*, 623−635.
(95) Bingman, C. A.; Zon, G.; Sundaralingam, M. *J. Mol. Biol.* **1992**, *227*, 738−756.
(96) van Dam, L.; Korolev, N.; Nordenskiöld, L. *Nucleic Acids Res.* **2002**, *30*, 419−428.
(97) Wolf, B.; Hanlon, S. *Biochemistry* **1975**, *14*, 1661−1670.
(98) Harmouchi, M.; Albiser, G.; Premilat, S. *Eur. Biophys. J.* **1990**, *19*, 87−92.

of the major groove. It should also explain the inability of poly(dA)·poly(dT) DNA to go to the A-form, which is perhaps due to the hydrophobic surface formed in the major groove by thymine methyl groups that affects the orientation freedom of a substantial part of water molecules and reduces the effective volume available to counterions. Modeling of these subtle effects, however, is likely to require further force field improvement especially as regards water−ion interactions. At the same time, we showed here that the water drop conditions present a very promising approach that can significantly facilitate further progress in this research direction.

Acknowledgment. The author gratefully acknowledges valuable comments to the manuscript from V. I. Ivanov and V. B. Zhurkin.

JA034550J